IEEE Access
Multidisciplinary ⋮ Rapid Review ⋮ Open Access Journal

Received 17 April 2023, accepted 10 May 2023, date of publication 15 May 2023, date of current version 24 May 2023.

Digital Object Identifier 10.1109/ACCESS.2023.3276715

RESEARCH ARTICLE

A Frequency-Domain I/Q Imbalance Calibration Algorithm for Wideband Direct Conversion Receivers Using Low-Cost Compensator

XIAOYE PENG[1], FAXIN YU[1], (Senior Member, IEEE), ZHIYU WANG[1], (Member, IEEE), JIARUI LIU[1], CHENGE WANG[1], AND JING WANG[2]

[1]School of Aeronautics and Astronautics, Institute of Astronautic Electronic Engineering, Zhejiang University, Hangzhou 310007, China
[2]Hangzhou Core Device Technologies Company Ltd., Hangzhou 310007, China

Corresponding author: Chenge Wang (wcghha@zju.edu.cn)

ABSTRACT The amplitude and phase imbalances of the in-phase (I) and quadrature (Q) branches inherent in the direct conversion receiver structure cause the generation of image frequency interference signals. In this paper, a frequency-domain I/Q imbalance calibration algorithm is proposed for wideband direct conversion receivers. The I/Q imbalance model is rebuilt by applying the infinitesimal method and FFT algorithm. The mathematical expressions for the exact computation of the I/Q imbalance parameters are derived based on the frequency-domain statistical properties of the baseband signal. The two phase parameters, frequency-dependent I/Q imbalance (FD-IQI) and frequency-independent I/Q imbalance (FI-IQI), are separated according to the parity properties of the imbalance parameter. To avoid the interference from the transmitter, the receiver impairment estimation is performed using a frequency offset (FO) DC training signal, and a low-cost real-valued compensation (RVC) filter is introduced to correct the impairments of the received signal. The performances of the proposed calibration model are evaluated through simulations and experiments. The simulation results show that the image rejection ratio (IRR) is improved to 80-120 dBc and can also exceed 40 dBc at high noise levels. The experimental results based on the CX9261A evaluation board show that the average IRR of the multi-tone signal is increased by 24.99 dB, and the IRR of the wideband signal is increased by 19.08 dB.

INDEX TERMS Direct conversion receiver, frequency-dependent I/Q imbalance, frequency-independent I/Q imbalance, frequency-domain statistical properties, infinitesimal method, real-valued compensation filter.

I. INTRODUCTION

Direct conversion transceivers have become the dominant approach to achieve large-bandwidth, high-integration, low-power, and low-cost transceiver designs in wideband radios [1]. In a direct conversion receiver, the received signal is directly quadrature down-converted from the radio frequency (RF) signal to a baseband signal. The topology of the direct conversion receiver includes a quadrature structure and in-phase (I) and quadrature (Q) branch channels. Its goal is to obtain two baseband signals with the same frequency, same amplitude, and phase difference of 90°. However, because of factors such as analog device mismatch, I/Q imbalance (IQI) is caused, which produces undesired image interference signals and affects the demodulation performance of the baseband signal [2].

The IQI in the wideband direct conversion receiver is caused by two different sources: (1) The frequency-independent (FI) amplitude and phase imbalances caused by the non-ideal analog quadrature mixer, (2) The frequency-dependent (FD) amplitude and phase imbalances caused by the differences between the two I/Q baseband analog paths, the analog paths including low-pass filter (LPF), analog to digital converter (ADC), and other devices. Neither of these I/Q imbalances can be ignored for wideband direct conversion receivers. Some references only use real-valued factors

The associate editor coordinating the review of this manuscript and approving it for publication was Young Jin Chun.

to compensate for IQI [3], [4], [5], [6]. However, when this compensation model is applied to wideband receivers, the entire baseband cannot achieve good image suppression. Therefore, they are more suitable for narrowband receivers. For wideband direct conversion receivers, it is generally necessary to use a digital filter to compensate for imbalance parameters. The structure of the algorithm determines the structure of the compensation filter. When the algorithm does not separate the FI and FD phase imbalance estimates, a complex-valued compensation (CVC) filter is required to compensate for IQI. The resource consumption of a CVC filter is equivalent to that of four real-valued compensation (RVC) filters. Therefore, the algorithm is preferred to separate the FI and FD phase imbalances, and then only one RVC filter is needed to compensate for the IQI which save resources.

At present, the IQI calibration algorithms of receiver are mainly divided into blind methods and training sequence methods according to whether data assistance is needed during calibration. In practical applications, blind methods are used for tracking calibration because of their blindness, and training sequence methods are used for power-on calibration because of the high-precision IQI parameter estimation of the entire baseband. A variety of RF transceivers developed by ADI company have IQI power-on calibration and blind tracking calibration functions, e.g. ADRV9002, ADRV9009, and AD9371.

Blind calibration does not require data assistance or other additional information, such as the modulation method of the signal. It uses only the inherent characteristics of the received signal to estimate channel imbalance parameters. References [2] [7], [8], [9], and [10] are related studies on blind calibration.

References [11], [12], [13], [14], [15], and [16] conducted relevant research on IQI calibration based on the training sequence method. A loopback path is required to send a designed training sequence before the useful signal, and then estimate the IQI parameters of the receiver. The algorithm proposed in this paper belongs to the training sequence method, so the relevant research on the training sequence method is introduced in detail. References [11], [12], [13], [14], [15], [16], [17], and [18] compensated the IQI with a CVC filter. In [11], Deng et al. studied transmitter and receiver wideband RF impairments based on the least squares (LS) algorithm. The CVC filter is equalized by four paralleled real-based filters. And frequency offset (FO) binary phase shift keying (BPSK) and quadrature phase shift keying (QPSK) training signals are used to calibrate the receiver and the transmitter, respectively. Lei et al. [12] used golay complementary sequence for receiver and used LS algorithm to iteratively estimate the CVC filter coefficients. In [13], Hsu and Sheen calibrated direct conversion transceivers based on the non-linear least squares (NLS) algorithm. Rosolowski and Korpas [14] used test monochromatic signals for training to perform ultrawideband receiver IQI calibration. Guan et al. [15] derived the calculation expressions of the IQI parameter according to the autocorrelation of the received signal and then sent the training sequence at N frequency points to estimate the IQI of the entire baseband. In [16], Aoki et al. used a multi-tone training signal. A phase shifter is inserted in the transceiver loopback path. Then the transmitter and receiver IQI can be estimated separately. Meanwhile, some studies have investigated the IQI compensation by a low-cost RVC filter [17], [18]. Nayebi et al. [17] proposed a new adaptive algorithm based on minimizing the Euclidean distance (ED) between the frequency-domain impaired signal and the known received reference signal. This scheme requires a large FFT size and is highly susceptible to noise levels. Liu et al. [18] used the least mean square (LMS) algorithm to iterate the transceiver the FD-IQI parameters and then used the conventional algorithm to calibrate the frequency-independent I/Q imbalance (FI-IQI). The loopback path for this model is complex, and requires a phase shifter and two analog selector switches. Using the analog selector switches during calibration introduces an additional IQI.

In this paper, a frequency-domain IQI calibration algorithm is proposed for wideband direct conversion receivers. Focusing on the training sequence method, we use an RVC filter to achieve compensation. And the IQI parameters are estimated in the frequency-domain for interference suppression of spurious signals. Our algorithm uses the properties of the baseband signal to directly calculate the imbalance parameters, and does not include the process of approximate estimation and iterative convergence. The algorithm still performs well in terms of calibration, even at high noise levels. The main contributions of this paper are summarized as follows.

1) This paper uses the infinitesimal method and FFT to rebuild the IQI model of a wideband receiver. Then, novel mathematical expressions for calculating the IQI parameters are derived based on the frequency-domain statistical properties of the baseband signals. Moreover, the FI and FD phase imbalance parameters are separated according to the parity properties of the imbalance parameter.
2) The FO-based DC signal is used as the training sequence of this model to avoid introducing additional imbalances of the transmitter. FO calibration tones can be obtained by tuning the local oscillator (LO) frequency of the transmitter.
3) We design a low-cost RVC structure, which includes an RVC filter, a delayer and two RVC factors. The IQI is removed by updating the coefficients in the structure.
4) The calibration scheme is applied to compensate for the RF impairments in the CX9261A evaluation board. Multi-tone and wideband test signals are employed to validate the performance of the image suppression improvement.

The following is a description of the symbols commonly used throughout this paper. The symbol $(\cdot)^*$ denotes

conjugation, $\otimes$ denotes convolution, $E[\cdot]$ denotes expectation, Re$[\cdot]$ denotes the real part, j denotes the imaginary unit.

II. I/Q IMBALANCE MODEL RECONSTRUCTION

A. COMPLEX WIDEBAND RECEIVER MODEL

In a non-ideal wideband direct conversion receiver, the mismatch between the two LO signals results in FI amplitude imbalance parameter g and the phase imbalance parameter φ. The mismatch of the I/Q baseband paths results in the FD amplitude imbalance parameter $M(f)$ and the phase imbalance parameter θ (f). Assume that h_I (t) and h_Q (t) are the impulse responses of the I/Q baseband paths respectively, and H_I (f) and H_Q (f) are the frequency-domain responses of h_I (t) and h_Q (t). The frequency response difference between I- and Q-branches is shown in (1). They can be compensated using a digital filter on either the I or Q paths.

$$\frac{H_Q(f)}{H_I(f)} = M(f)e^{j\theta(f)}. \tag{1}$$

We use the received mismatch training sequence to estimate the IQI parameters; therefore, it is important to establish a complete signal model. First, we assume $z(t) = z_I(t) + jz_Q(t)$ is an ideal baseband signal, f_c is the carrier frequency, and the expression for the received RF signal $r(t)$ is

$$r(t) = 2Re\left[z(t)e^{j2\pi f_c t}\right]. \tag{2}$$

The received RF signal first passes through the quadrature mixer, and then transforms into the baseband signal through the LPF and ADC. The mathematical model for this process is

$$\begin{aligned} x(t) &= \{r(t)\cos 2\pi f_c t\} \otimes h_I(t) \\ &\quad + j\{r(t)[-g\sin(2\pi f_c t + \varphi)]\} \otimes h_Q(t) \\ &= z(t) \otimes \frac{1}{2}\left[h_I(t) + ge^{-j\varphi}h_Q(t)\right] \\ &\quad + z(t)^* \otimes \frac{1}{2}\left[h_I(t) - ge^{j\varphi}h_Q(t)\right]. \end{aligned} \tag{3}$$

Equation (3) is the mathematical model of the baseband signal received by a non-ideal wideband direct conversion receiver, which includes four imbalanced parameters with different characteristics. The wideband receiver model is complex, so it is difficult to directly calculate each imbalance parameter. We will rebuild the IQI model in subsection II-B.

As in [11] and [13], the frequency-domain image rejection ratio (IRR) is defined as the ratio of the spectral energy of the useful signal to the spectral energy of the image signal, and is used to describe the non-ideality of the signal. It can be written as

$$IRR(f) = 10\log_{10}\frac{|G_1(f)|^2}{|G_2(f)|^2}. \tag{4}$$

where

$$\begin{cases} G_1(f) = \frac{1}{2}\left[H_I(f) + ge^{-j\varphi}H_Q(f)\right], \\ G_2(f) = \frac{1}{2}\left[H_I(f) - ge^{j\varphi}H_Q(f)\right]. \end{cases} \tag{5}$$

B. REBUILD I/Q IMBALANCE MODEL

Generally, the frequency responses H_I (f) and H_Q (f) of the analog baseband paths are non-abrupt, and the response curves of the amplitude and phase change steadily with the baseband frequency. Based on the infinitesimal method, we divide the baseband frequency into K parts and assume that the amplitude imbalance parameter M (f) and phase imbalance parameter θ (f) in the $k0$ segment are stable constants. We solve the IQI problem of the whole baseband by analyzing the imbalance in a certain frequency range.

Suppose the ideal baseband signal at frequency f_0 is

$$\begin{cases} z_I(t) = \cos 2\pi f_0 t, \\ z_Q(t) = \sin 2\pi f_0 t. \end{cases} \tag{6}$$

Then the mathematical model of the baseband signal with frequency f_0 received by the receiver is

$$\begin{cases} x_I(t) = \cos 2\pi f_0 t \otimes h_I(t), \\ x_Q(t) = g\sin(2\pi f_0 t - \varphi) \otimes h_Q(t). \end{cases} \tag{7}$$

We assume that at a certain frequency f_0 in the baseband band, the amplitude and phase imbalances of the Q path relative to the I path are M_0 and θ_0 respectively. Then incorporate the FD-IQI parameters into the FI-IQI parameters $\alpha_0 = gM_0$, $\beta_0 = \varphi - \theta_0$. Equation (7) can be simplified as

$$\begin{cases} x_I(t) = \cos 2\pi f_0 t \otimes h_I(t), \\ x_Q(t) = \alpha_0\sin(2\pi f_0 t - \beta_0) \otimes h_I(t). \end{cases} \tag{8}$$

In (8), both the I/Q signals are convolved with h_I (t) without introducing additional amplitude and phase mismatch, so we set h_I $(t) = 1$. In order to facilitate the derivation and description of the algorithm below, we substitute (6) back into (8) to obtain (9), and (9) is the rebuilt wideband receiver IQI time-domain mathematical model. Because the signals processed in the digital domain are all discrete, the expressions we deduce below are all written as discrete expressions.

$$\begin{cases} x_I(n) = \frac{1}{2}\left[z(n) + z^*(n)\right], \\ x_Q(n) = \frac{\alpha_0}{2j}\left[z(n)e^{-j\beta_0} - z^*(n)e^{j\beta_0}\right]. \end{cases} \tag{9}$$

III. FREQUENCY-DOMAIN I/Q IMBALANCE CALIBRATION ALGORITHM

In this section, we propose an IQI calibration algorithm based on the frequency-domain statistical properties of the baseband signal. A block diagram of the calibration model is shown in Fig. 1, in which the RVC architecture is used as the compensator. The calculation of the filter coefficients $h[n]$ and compensation factor φ is the key to IQI calibration.

This IQI calibration algorithm is suitable for the power-on calibration of direct conversion transceivers. As shown in Fig. 1, the loopback path structure is simple and does not require additional analog devices such as phase shifters. In the receiver IQI calibration procedure, the digital signal generator sends the DC signal to the transmitter, and then the RF signal output by the transmitter is looped back to the receiver from

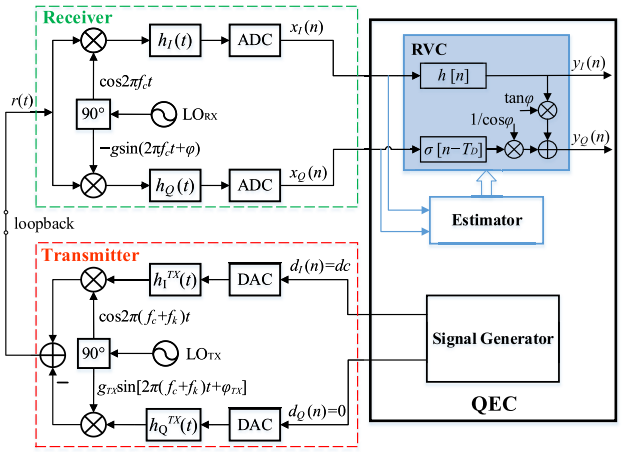

FIGURE 1. Schematic diagram of loopback calibration.

the RF end. There is a frequency difference between the LO of the receiver and transmitter. We assume that the LO frequency of the receiver is f_c, and the baseband target calibration frequency is f_k, then LO frequency of the transmitter is $f_c + f_k$.

As shown in (10), using the DC signal as the training sequence does not add additional IQI characteristics of the transmitter.

$$r(t) = dc \otimes h_I^{TX}(t) \cos\left[2\pi(f_c + f_k)t\right]. \tag{10}$$

The baseband signal received by the receiver is a single-tone signal with frequency f_k, which is the calibration tone. The calibration tone data stream is passed to the estimator, which uses the information at the calibration tone f_k to estimate the IQI parameters. After estimating the imbalance parameters at all the target calibration frequencies, the estimator updates the compensation coefficients to the RVC. The power-on calibration is complete.

Fig. 2 shows the estimation process of the IQI calibration algorithm proposed in this paper. The following subsections mainly introduce the data preprocessing, algorithm derivation and RVC design, as shown in Fig. 2.

A. DATA PREPROCESSING

Data preprocessing mainly involves grouping, windowing, FFT, and sampling of the received baseband signal to reduce the influence of energy leakage on the estimation accuracy of subsequent algorithms. First, the received data are grouped. Assuming that there are $P = N \times W$ data, which are divided into W groups, each group contains N data. The amount of data N in each group determines the length of FFT, the length of the RVC filter coefficient, and also the location of the frequency points. In this paper, we call these frequency points calibration points. Assuming f_s is the sampling rate of the baseband signal, the number of calibration points is N–2, and they are evenly distributed over the entire frequency band. The frequency calculation equation for each calibration point is (11). When the signal frequency is 0 or $f_s/2$, it is difficult to separate the overlapping image from the signal; therefore, we do not calculate the IQI parameters at $k = 0$ and $k = N/2$, and use the estimated parameters of adjacent calibration points instead.

$$f_k = \frac{kf_s}{N}, \quad k = 1, \ldots, \frac{N-1}{2}, \frac{N+1}{2}, \ldots N-1. \tag{11}$$

Our proposed model calculates the imbalance parameter at the calibration points; therefore, the amplitude spectrum accuracy at the calibration frequency must be high. However, the signal spectrum leakage will greatly affect the accuracy of the calculation, and it is necessary to select a window function with small a side lobe peak value, large attenuation amplitude, and fast attenuation to reduce the spectrum leakage [19]. The Blackman window is selected because it has lower side lobe levels than most other windowing functions [18]. After windowing, the data are subjected to FFT to obtain the corresponding frequency-domain data matrix.

We use single-tone signals as the calibration tones. To avoid in-band spurs affecting the estimation accuracy of IQI parameters, in the sampling process, we only take information X_I and X_Q at the current calibration point f_k and its image $N - f_k$ to calculate the imbalance parameters at the corresponding frequency. Only the imbalance parameter at the current frequency f_k is calculated each time, and the LO frequency is adjusted $N - 2$ times to obtain the imbalance parameter of the entire baseband.

B. A NOVEL I/Q IMBALANCE CALIBRATION ALGORITHM

We conducted related research on IQI calibration and derived novel mathematical expressions for calculating the IQI parameters α, φ and θ. This algorithm can accurately calculate the imbalance parameters of wideband receivers and achieve a significant calibration effect. The derivation process of this algorithm is described below.

Equation (9) is converted into a frequency-domain expression based on Fourier transform. The Fourier transform does not change the amplitude or phase of the signal and can separate the frequency components of the signal [20]. Then, the mathematical model of the IQI signal in the k_0th frequency band is

$$\begin{cases} X_I(k_0) = \dfrac{1}{2}[Z(k_0) + Z^*(N-k_0)], \\ X_Q(k_0) = \dfrac{\alpha_0}{2j}\left[Z(k_0)e^{-j\beta_0} - Z^*(N-k_0)e^{j\beta_0}\right]. \end{cases} \tag{12}$$

In related research on IQI calibration using the frequency-domain statistical properties of the baseband signal, some studies infer that the ideal baseband signal $Z(k)$ is uncorrelated in the frequency-domain and satisfies the following (13) [10]:

$$\begin{cases} E[Z(k)Z(N-k)] = 0, \\ E[Z^*(k)Z^*(N-k)] = 0, \\ E[Z(k)Z^*(N-k)] = 0, \\ E[Z^*(k)Z(N-k)] = 0. \end{cases} \tag{13}$$

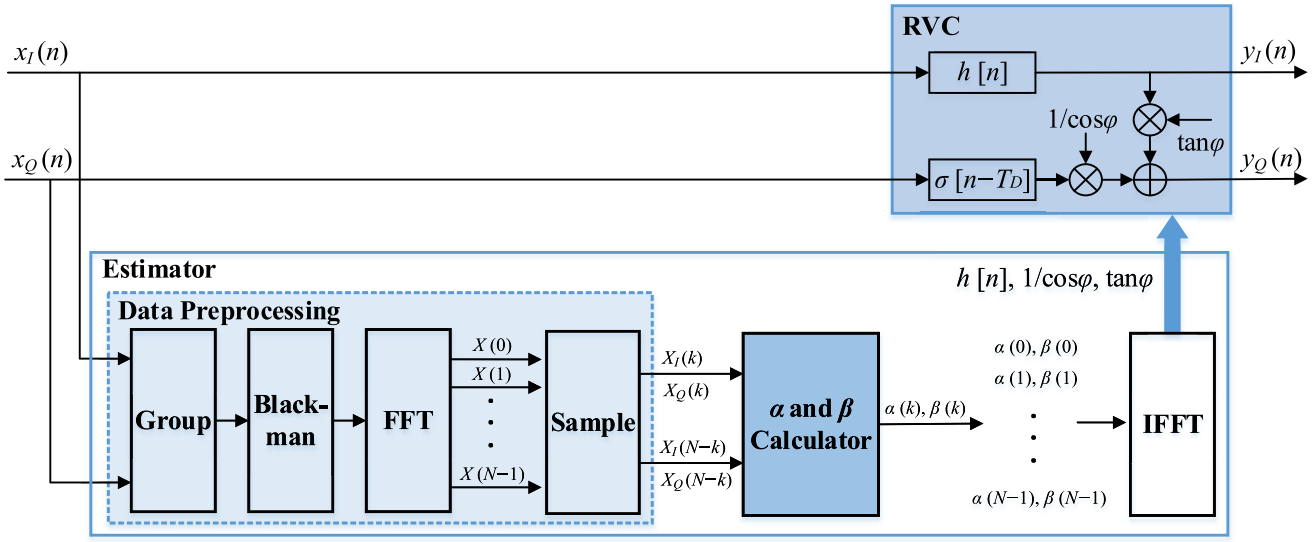

FIGURE 2. Schematic diagram of loopback calibration.

Based on the rebuilt IQI model and frequency-domain statistical properties introduced above, we conduct the following derivations to solve for the IQI parameters.

We combine the expressions of I/Q paths in (12), deform them, and substitute (13) for simplification to obtain (14)-(17). Then, the following equations are used to calculate the imbalance parameters, α_0 and β_0.

$$E[X_I(k_0)X_I^*(k_0)] = \frac{1}{4}\left\{E[Z(k_0)Z^*(k_0)] + E[Z(N-k_0)Z^*(N-k_0)]\right\}, \tag{14}$$

$$E[X_Q(k_0)X_Q^*(k_0)] = \frac{\alpha_0^2}{4}\left\{E[Z(k_0)Z^*(k_0)] + E[Z(N-k_0)Z^*(N-k_0)]\right\}, \tag{15}$$

$$E[X_I^*(k_0)X_Q(k_0)] = \frac{\alpha_0}{4j}\left\{E[Z(k_0)Z^*(k_0)]e^{-j\beta_0} - E[Z(N-k_0)Z^*(N-k_0)]e^{j\beta_0}\right\}, \tag{16}$$

$$E[X_I^*(N-k_0)X_Q(N-k_0)] = \frac{\alpha_0}{4j}\left\{E[Z(N-k_0)Z^*(N-k_0)]e^{-j\beta_0} - E[Z(k_0)Z^*(k_0)]e^{j\beta_0}\right\}. \tag{17}$$

By dividing (15) by (14) and taking its root, we obtain (18) to calculate the amplitude imbalance parameter α_0. $X_I(k_0)$ and $X_Q(k_0)$ are the I/Q calibration tones received by the receiver, respectively.

$$\alpha_0 = \sqrt{\frac{E[X_Q(k_0)X_Q^*(k_0)]}{E[X_I(k_0)X_I^*(k_0)]}}. \tag{18}$$

Adding (16) to (17) and dividing by (14) to obtain (19), α_0 can be calculated by (18), then the phase imbalance parameter β_0 can be calculated by

$$\beta_0 = -\arcsin\left\{\frac{E[X_I^*(k_0)X_Q(k_0)]}{2\alpha_0 E[X_I(k_0)X_I^*(k_0)]} + \frac{E[X_I^*(N-k_0)X_Q(N-k_0)]}{2\alpha_0 E[X_I(k_0)X_I^*(k_0)]}\right\}. \tag{19}$$

By generalizing the above mathematical expression for the entire baseband, (18) and (19) can be written as

$$\alpha(k) = \sqrt{\frac{E[X_Q(k)X_Q^*(k)]}{E[X_I(k)X_I^*(k)]}}, \tag{20}$$

$$\beta(k) = -\arcsin\left\{\frac{E[X_I^*(k)X_Q(k)]}{2\sqrt{E[X_I(k)X_I^*(k)]E[X_Q(k)X_Q^*(k)]}} + \frac{E[X_I^*(N-k)X_Q(N-k)]}{2\sqrt{E[X_I(k)X_I^*(k)]E[X_Q(k)X_Q^*(k)]}}\right\}. \tag{21}$$

In this mathematical model, the amplitude imbalance parameter α includes the FI and FD amplitudes and the phase imbalance parameter β includes the FI and FD phases. According to the frequency response characteristics of the real-valued filter, we must separate the two phase imbalance parameters. The FD phase imbalance parameter is an odd function and the FI phase imbalance parameter is a constant. Therefore, we average the calculated phase imbalance parameters at the baseband positive and negative symmetrical frequency points to separate the FI phase imbalance parameter.

$$\bar{\varphi} = \frac{1}{N-2}\left(\sum_{k=1}^{N/2-1}\beta(k) + \sum_{k=N/2+1}^{N-1}\beta(k)\right). \tag{22}$$

Then the equation for calculating the FD phase imbalance parameter θ is

$$\theta(k) = \bar{\varphi} - \beta(k). \tag{23}$$

C. RVC DESIGN

According to Euler's formula [21], we write (3) equivalently as

$$\begin{aligned} x(n) &= x_I(n) + jx_Q(n) \\ &= z_I(n) \otimes h_I(n) \\ &\quad + j\left[z_Q(n)\cos\varphi - z_I(n)\sin\varphi\right] \otimes h_Q(n). \end{aligned} \tag{24}$$

From (24), the RVC structure can be obtained as shown in Fig. 2. It comprises a pure delay unit on the Q path and an RVC filter on the I path, denoted by $h[n]$. The RVC digital filter is used to compensate for the amplitude imbalance and FD phase imbalance between the I and Q paths. The filter causes a group delay of data; therefore, the delay unit on the Q path is used to achieve synchronization with the I path. Suppose that the length of $h[n]$ is N, the delay unit on the Q path is denoted by T_D, and its value is $N/2$. The imbalance parameter φ is added to the I- and Q-branches to compensate for the FI phase imbalance.

The compensated signal $y(n) = y_I(n) + jy_Q(n)$ at the output of the RVC is given by

$$\begin{cases} y_I(n) = x_I(n) \otimes h(n), \\ y_Q(n) = x_Q(n - T_D)\dfrac{1}{\cos\varphi} + x_I(n) \otimes h(n)\tan\varphi. \end{cases} \tag{25}$$

Through the analysis of subsection III-B, we deduce the mathematical model of the amplitude imbalance parameter α, the FD phase imbalance parameter θ, and the FI phase imbalance parameter φ. Then the RVC filter coefficients can be easily calculated by

$$h[n] = Re\left\{IFFT\left[\alpha e^{j\theta}\right]\right\} \tag{26}$$

IV. SIMULATIONS

To verify the model mentioned in this paper, we cite two test cases in [9] and [11] for simulation and compared the calibration effect of this model and [11]. The FI amplitude imbalance $g = 0.7$, and the phase imbalance $\varphi = -2°$. The FD-IQI parameters are as follows:

- Case 1: $h_I = [0.95\ -0.3\ 0.15\ -0.08]$, $h_Q = [1\ -0.2\ 0.1\ 0.06]$.
- Case 2: $h_I = [0.98, 0.03]$, $h_Q = [1, -0.005]$.

In the proposed model, the greater the number of calibration points chosen, the more information about the IQI of the receiving analog channel that is captured. The following selects different lengths of the RVC filter coefficient N = 32, 64, 128, and 256 for the simulation. In the simulations, $f_s = 122.88$ MHz. Under different configuration conditions, MATLAB [22] is used to generate the calibration tones, and Gaussian white noise and IQI are added. After the imbalance parameters are estimated, a frequency-sweep test is performed (single-tone signals with IQI, [−60:5:60] MHz). The statistical number of each calibration tones used in each simulation is 32768. The simulation results are shown in Fig. 4.

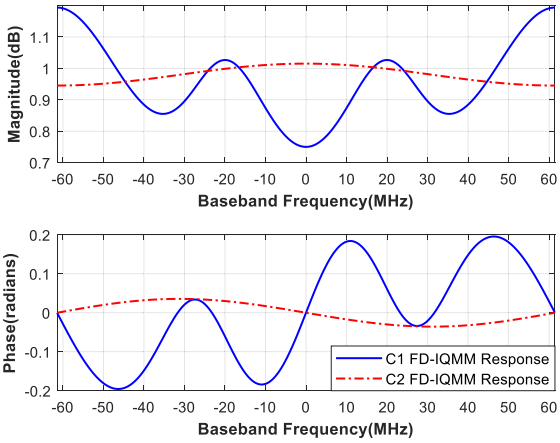

FIGURE 3. The amplitude-frequency response curves and phase-frequency response curves of FD-IQI of Case1 and Case2.

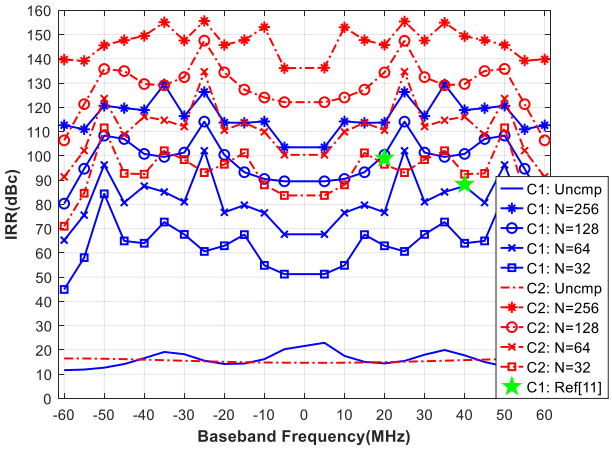

FIGURE 4. Spectral IRR performance of the IQI Cases (C1/C2) in the baseband before and after compensation under noise-free conditions.

The simulation results of [11] under noise-free conditions are indicated by green stars in Fig. 4. After calibration, the IRR is 99.011 dBc at 20 MHz (before calibration is 14.4348 dBc) and 88.238 dBc at 40 MHz (before calibration is 17.7352 dBc). Under the same simulation conditions as [11], the simulation results for the algorithm proposed in this paper are shown in Fig. 4. When $N = 128$, the IRR after compensation at 20 MHz is 100.40 dBc, and the IRR after compensation at 40 MHz is 100.77 dBc. The calibration effects of these two frequency points is better than [11].

Fig. 4 shows that for the proposed model, the longer the coefficient length of the RVC filter, the higher the IRR. When the length of the RVC filter coefficient reaches a certain level, the IRR no longer increases significantly. When $N = 32$, the simulation results of the proposed model are IRRC1 = 44.91-84.33 dBc, IRRC2 = 70.97-111.52 dBc. When $N = 128$,

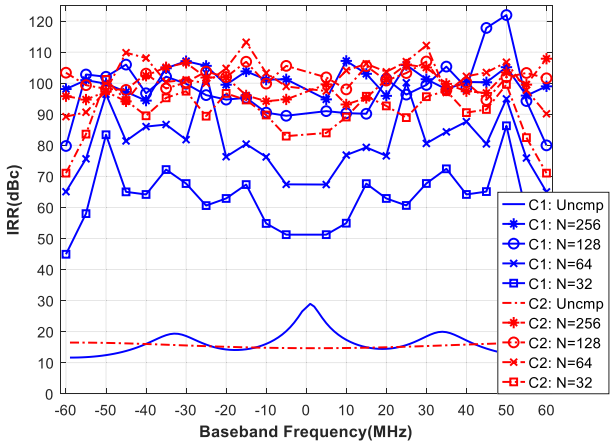

FIGURE 5. Spectral IRR performance of the IQI Cases (C1/C2) in the baseband before and after compensation under 60dB SNR.

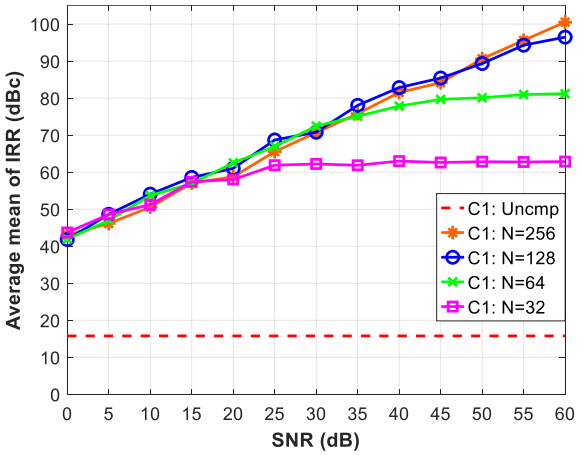

FIGURE 6. Average mean of IRR versus SNR for Case1. When SNR = 0dB, the average mean of IRR all exceeds 40dBc.

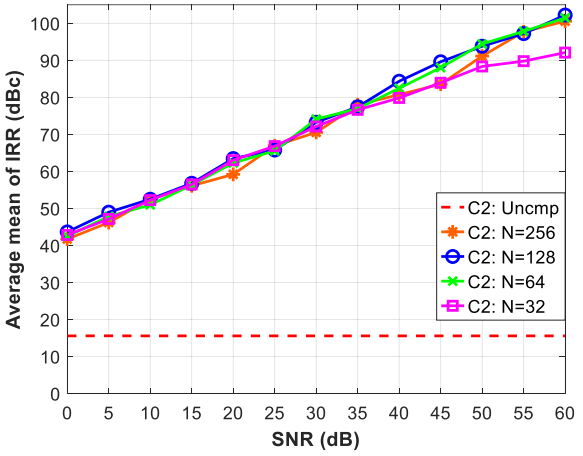

FIGURE 7. Average mean of IRR versus SNR for Case2. When SNR = 0dB, the average mean of IRR all exceeds 40dBc.

the simulation results of the proposed model are IRRC1 = 80.26-114.09 dBc, IRRC2 = 106.37-147.46 dBc. Combined with the simulation results in Fig. 3, we can see that different FD-IQI have different requirements for the RVC filter coefficient length. The frequency response curve of the FD-IQI of Case1 is relatively complex and steep; therefore, more RVC filter coefficients ($N = 128$) are needed to achieve a good IQI calibration effect for the entire baseband (most IRR over 80 dBc). However, the frequency response curve of the FD-IQI of Case2 is simple and smooth, and thus, 32 RVC filter coefficients can achieve a high IRR (most IRR over 80 dBc). Since the FD-IQI of a direct conversion receiver is caused by factors such as tape-out process and device mismatch, it is difficult to determine the complexity of the FD-IQI frequency response curve, so it is difficult to accurately know the coefficient length of the RVC filter in advance.

The above simulation is carried out under the condition of no noise, but the transmission process of the signal in the actual direct conversion receiver is accompanied by noise. When the signal-to-noise ratio (SNR) is set to 60 dB, the simulation results of the algorithm in this paper are shown in Fig. 5. Comparing Fig. 5 with Fig. 4 shows that noise limits calibration performance.

We also performed simulations of the sensitivity of the algorithm to noise level. We estimate the imbalance parameters at different SNRs and performed frequency-sweep tests (single-tone signals with IQI, [−60:5:60] MHz) and averaged the tested IRR. Fig. 6 and Fig. 7 show the average mean of IRR versus SNR at different length of the RVC filter coefficient $N = 32$, 64, 128, and 256.

In Fig. 6 and Fig. 7, we observe that the IRR increases with the SNR. In Fig. 6, when the SNR increases above 30dB, the simulation result curves for $N = 32$ and 64 gradually converge. Because the RVC filters with these two coefficient lengths cannot adapt well to the frequency response curve of Case1, the calibration effect is limited. The algorithm proposed in [17] is highly sensitive to the noise level, and when the SNR is lower than 20 dB, the calibration is failed. While our algorithm still exhibits a good calibration effect under a low SNR.

V. EXPERIMENTS

In addition to the simulation, we build a hardware and software co-testing platform to verify the effectiveness of our proposed algorithm. The experimental environment is illustrated in Fig. 8. MATLAB [22] is used to build the IQI calculation model to handle the received calibration tones. The hardware modules include the Hangzhou Core Device Technologies company's CX9261A Evaluation Board, Xilinx's Zynq Evaluation Platform (EK-Z7-ZC706-G), two RF signal generators, and a Power Supply (GPD-4303S). CX9261A is the experimental object, which is a wideband RF transceiver. CX9261A can work in frequency division duplexing (FDD) mode, and the digital channel of the chip includes an IQI compensation module, and the user can configure compensation coefficients independently through the AHB Bus.

TABLE 1. Comparison of algorithms, performance, compensators between this work and others.

			Proposed	[11]	[12]	[13]
Estimation Model			Direct calculation based on frequency-domain statistical properties	LS and iterative	LS and iterative	NLS and iterative
Domain of the algorithm			Frequency	Time	Time	Time
Compensator structure			A real-valued filter and two real factors	Four real-valued filters	Two real-valued filters	A complex-valued filter
[11] Case	No noise	IRR(dBc) at 20 MHz	100.40	99.01	-	-
	No noise	IRR(dBc) at 40 MHz	100.77	88.24	-	-
[12] Case	SNR=10 dB	Average IRR(dBc)	52.77	-	32.06	-
	SNR=20 dB	Average IRR(dBc)	62.59	-	42.14	-
[13] Case	SNR=35 dB	IRR(dBc) at 4 MHz	79.76	-	-	50.80
	SNR=45 dB	IRR(dBc) at 4 MHz	85.97	-	-	60.80
	SNR=55 dB	IRR(dBc) at 4 MHz	89.70	-	-	70.80

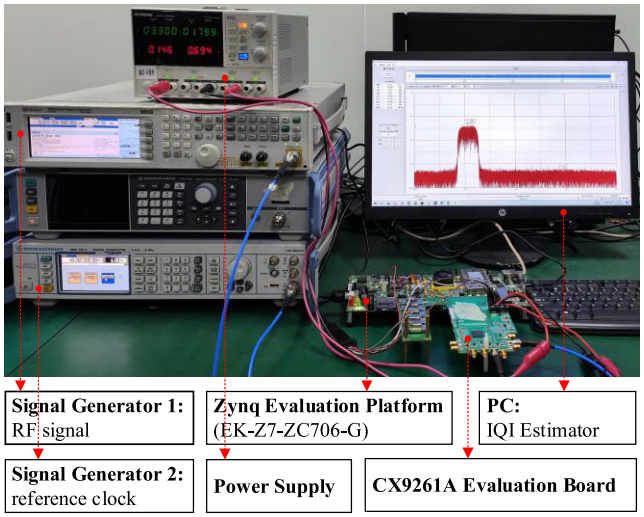

FIGURE 8. Measurement platform of CX9261A loopback calibration.

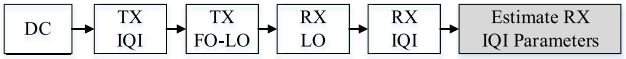

FIGURE 9. Calibration and verification flows of the loopback transceiver.

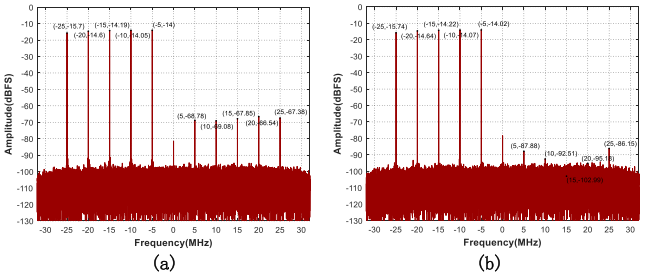

FIGURE 10. The amplitude spectra of multi-tone signal: (a) the mean of IRR before compensation is 53.42dBc; (b) the mean of IRR after compensation is 78.41dBc. The RVC filter coefficient length N = 32.

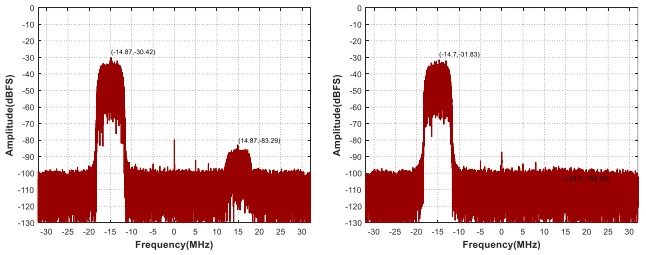

FIGURE 11. The amplitude spectra of wideband signal: (a) IRR = 52.87dBc before compensation; (b) IRR = 71.95dBc after compensation. The RVC filter coefficient length N = 32.

The experimental link process is shown in Fig. 9. We turned off the IQI calibration enable switch of CX9261A. The baseband output DC signal is passed through the transmitter and loops back from the RF end to the receiver (LORX = 3 GHz), and the FO calibration tone is obtained by configuring different transmitter LO frequencies (LOTX = 3 GHz + fk). We use the MATLAB to edit the script to call the function provided by the Hangzhou Core Device Technologies company to read the memory (SDRAM) data of the Zynq evaluation platform. The IQI estimation model built in MATLAB calculates the imbalance parameters of the receiver according to the data of each calibration tone, and finally configures the internal IQI compensation module of CX9261A through the AHB bus to realize the calibration of the receiver.

We test the compensation coefficients with multi-tone and wideband signals: (1) the signal generator sends a set of multi-tone signals with a frequency interval of 5 MHz, center frequency of 3.015 GHz, and amplitude of −20 dBm. (2) The signal generator sends a wideband signal with a modulation mode of QPSK, configured with a roll-off factor of 0.35, symbol transmission rate of 5 Msps, center frequency of 3.015 GHz, and amplitude of −20 dBm.

Fig. 10 and Fig. 11 show the amplitude spectra of the multi-tone and wideband signals before and after IQ compensation, respectively. The average IRR of the multi-tone signal before compensation is 53.42 dBc, and the average IRR after compensation is 78.41 dBc (with 24.99 dB improvement). The wideband signal has the largest amplitude at 14.87 MHz before compensation, with an IRR of 52.87 dBc. Since the received signal is dynamic, the wideband signal captured after compensation shown in the paper has the maximum energy at 14.7MHz, and the IRR after compensation at this frequency is 71.95 dBc (with 19.08 dB improvement). The above experimental results show a good calibration effect of the proposed IQI calibration model on both multi-tone and wideband signals.

VI. CONCLUSION

In this paper, we have proposed an IQI calibration algorithm and designed an RVC structure to realize IQI compensation of the wideband direct conversion receiver. First, we use the FO-based DC signal as the training sequence for this calibration to avoid introducing additional imbalances of the transmitter. We rebuild the IQI model of the wideband receiver based on the infinitesimal method and FFT. Based on the frequency-domain statistical properties of the baseband signal, we derive the novel mathematical expressions for the exact computation of the IQI parameters. After the imbalance parameter estimation for the entire baseband is completed, the FI and FD phase imbalance parameters are separated according to the parity properties of the imbalance parameter. We use MATLAB to build an IQI calibration model for simulation and experimentation. The simulation results show an IRR improvement to 80-120 dBc, and the IRR exceeds 45 dBc even when the SNR is 5 dB. The experimental results exhibit an IRR improvement of both multi-tone and wideband signals to approximately 20 dB. Finally, we conduct additional simulation experiments on our algorithm using the test cases of [12] and [13], and compare our calibration algorithm with other training sequence methods in detail, as shown in Table 1. The algorithm can accurately calculate the IQI parameters of the wideband direct conversion receiver, and can realize IQI compensation only by using a low-cost RVC.

ACKNOWLEDGMENT

The authors would like to thank the Institute of Aerospace Electronics Engineering, Zhejiang University, for providing the research platform and technical support.

REFERENCES

[1] Y. Wu, "Research on direct-conversion technology for radar application," *J. Electron. Inf. Technol.*, vol. 43, pp. 1170–1176, 2021.
[2] X. Peng, Z. Wang, J. Mo, C. Wang, J. Liu, and F. Yu, "A blind calibration model for I/Q imbalances of wideband zero-IF receivers," *Electronics*, vol. 9, no. 11, p. 1868, Nov. 2020.
[3] S. W. Ellingson, *Correcting IQ Imbalance in Direct Conversion Receivers*. London, U.K.: Argus Technical and Scientific Documents, 2003.
[4] P. Rykaczewski and F. Jondral, "Blind I/Q imbalance compensation in multipath environments," in *Proc. IEEE Int. Symp. Circuits Syst.*, May 2007, pp. 29–32.
[5] C. Zekkari, M. Djendi, and A. Guessoum, "IQ imbalance estimation and compensation in receiver system," in *Proc. Int. Conf. Adv. Electr. Eng. (ICAEE)*, Nov. 2019, pp. 1–5.
[6] Y. Luo, W. Li, and X. Hou, "A joint estimation and independent compensation scheme for transmitter and receiver IQ imbalance in zero-IF transceivers," in *Proc. IEEE Int. Conf. Comput. Electromagn. (ICCEM)*, Mar. 2019, pp. 1–5.
[7] L. Anttila, M. Valkama, and M. Renfors, "Circularity-based I/Q imbalance compensation in wideband direct-conversion receivers," *IEEE Trans. Veh. Technol.*, vol. 57, no. 4, pp. 2099–2113, Jul. 2008.
[8] L. Anttila and M. Valkama, "Blind signal estimation in widely-linear signal models with fourth-order circularity: Algorithms and application to receiver I/Q calibration," *IEEE Signal Process. Lett.*, vol. 20, no. 3, pp. 221–224, Mar. 2013.
[9] M. Petit and A. Springer, "Analysis of a properness-based blind adaptive I/Q filter mismatch compensation," *IEEE Trans. Wireless Commun.*, vol. 15, no. 1, pp. 781–793, Jan. 2016.
[10] A. Wei, R. Brian, and P. S. Richard., "Real-time I/Q imbalance correction for wide-band RF receiver," U.S. Patent US10 050 744 B2, Aug. 14, 2018.
[11] J. Deng, C. Lee, M. Ku, and J. Hwang, "Self-calibration of joint RF impairments in a loopback wideband transceiver," *IEEE Access*, vol. 8, pp. 45607–45617, 2020.
[12] C. Lei, L. Zhigang, C. Xiantao, and L. Shaoqian, "Golay sequence based time-domain compensation of frequency-dependent I/Q imbalance," *China Commun.*, vol. 11, no. 6, pp. 1–11, Jun. 2014.
[13] C.-J. Hsu and W.-H. Sheen, "Joint calibration of transmitter and receiver impairments in direct-conversion radio architecture," *IEEE Trans. Wireless Commun.*, vol. 11, no. 2, pp. 832–841, Feb. 2012.
[14] D. W. Rosolowski and P. Korpas, "IQ-imbalance and DC-offfset compensation in ultrawideband zero-IF receiver," in *Proc. 23rd Int. Microw. Radar Conf. (MIKON)*, Oct. 2020, pp. 209–213.
[15] S. Guan, D. Cai, and B. Wu, "Estimation and correction of I/Q imbalance in wideband zero-IF receiver," in *Proc. Int. Conf. Inf. Technol. Comput. Appl. (ITCA)*, Dec. 2019, pp. 50–54.
[16] Y. Aoki, M. T. Dao, K. Min, Y. Hwang, Y. Kim, and S. Yang, "1.4-GHz bandwidth frequency-dependent I/Q imbalance calibration for 5G mmWave communications," in *IEEE MTT-S Int. Microw. Symp. Dig.*, Jun. 2019, pp. 626–629.
[17] E. Nayebi, P. Dayal, and K. Song, "Adaptive IQ mismatch compensation in time-domain using frequency-domain observations," *IEEE Trans. Signal Process.*, vol. 69, pp. 655–668, 2021.
[18] Z. Liu, J. Wang, and Y. Wang, "Low-complexity calibration of joint TX/RX I/Q imbalance in wideband direct-conversion transceiver," in *Proc. IEEE Int. Symp. Broadband Multimedia Syst. Broadcast. (BMSB)*, Oct. 2020, pp. 1–5.
[19] V. Alan, S. Oppenheim Alan, S. Willsky, and N. Hamid, *Signals and Systems*, 2nd ed. Bejing, China: Publishing House of Electronics Industry, 2013, p. 238.
[20] J. G. Proakis and D. G. Manolakis, *Digital Signal Processing Principle, Algorithms, and Applications*, 4nd ed. Beijing, China: Publishing House of Electronics Industry, 2018, pp. 200–204.
[21] D. Wang, G.-J. Nian, and K. Wang, "Euler's formula in computing hypercomplex Fourier transform," in *Proc. 4th Int. Congr. Image Signal Process.*, Oct. 2011, pp. 755–759.
[22] V. K. Ingle and J. G. Proakis, *Digital Signal Processing using MATLAB*, Xian, China: Xian Jiaotong Univ. Press, 2018, pp. 258–264.

XIAOYE PENG was born in Sanmenxia, Henan, China, in 1996. She received the B.S. degree from China Jiliang University, Hangzhou, China, in 2018. She is currently pursuing the Ph.D. degree with Zhejiang University. Her current research interests include RF calibration, digital chip design, and software-defined radios.

FAXIN YU (Senior Member, IEEE) received the B.S., M.S., and Ph.D. degrees in communication and information systems from the Harbin Institute of Technology, Harbin, China. He used to work with UTStarcom Company. He is currently a Qiushi Distinguished Professor and a Doctoral Supervisor with Zhejiang University. He developed a large number of high-end radio frequency analog chips used in communications, navigation, and radar. He has published more than 60 SCI papers and more than 20 patents.

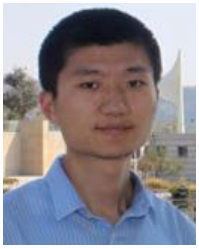

ZHIYU WANG (Member, IEEE) received the B.S. degree in information engineering and the Ph.D. degree in electromagnetic field and microwave technology from Zhejiang University, Hangzhou, China, in 2007 and 2013, respectively. He was a Lecturer with Zhejiang University, in 2013, and promoted to an Associate Professor, in 2015. In 2011 and 2012, he was a Visiting Student with the Research Laboratory of Electronics (RLE), Massachusetts Institute of Technology (MIT), and the Harvard School of Engineering and Applied Sciences. He is also committed to scientific research and technical applications in the frontier and hot fields of electromagnetic waves. He has published more than 20 scientific papers and U.S. patents.

JIARUI LIU received the Graduate degree from the School of Information and Electronic Engineering, Zhejiang University, Hangzhou, China, in 2009, and the Ph.D. degree in aerospace information technology from Zhejiang University, in 2014. In 2014, he entered the postdoctoral mobile station with Zhejiang University to study, where he left the station and joined the Institute of Aerospace Electronics Engineering, in 2016. He promoted to an Associate Researcher, in 2018. He is committed to the design and industrialization of digital-analog hybrid integrated circuits.

CHENGE WANG was born in Hangzhou, Zhejiang, China, in 1988. He received the Ph.D. degree in measurement technology and instruments from Zhejiang University, Hangzhou, in 2017. In October 2017, he entered the postdoctoral station in optical engineering with Zhejiang University to study and research, where he left the station and joined the Institute of Aerospace Electronics Engineering, in March 2020.

JING WANG was born in Jinxiang, Shandong, China, in 1983. She received the M.S. degree in physical electronics from Yunnan University, Kunming, China, in July 2012. From 2012 to 2018, she worked in the direction of radar signal processing with Guizhou Aerospace Electronics Technology Company Ltd. Since April 2018, she has been engaged in the research of signal processing, QEC, DPD, and other algorithms with Hangzhou Core Device Technologies Company Ltd.